Mathematics Interdisciplinary Research **9** (4) (2024) 425 − 442

Original Scientific Paper

Solving Linear and Nonlinear Duffing Fractional Differential Equations Using Cubic Hermite Spline Functions

*Mehrdad Lakestani** and *Roya Ghasemkhani*

Abstract

In this work, we solve nonlinear Duffing fractional differential equations with integral boundary conditions in the Caputo fractional order derivative sense. First, we introduce the cubic Hermite spline functions and give some properties of these functions. Then we make an operational matrix to the fractional derivative in the Caputo sense. Using this matrix and derivative matrices of integers (first and second order) and applying collocation method, we convert nonlinear Duffing equations into a system of algebraic equations that can be solved to find the approximate solution. Numerical examples show the applicability and efficiency of the suggested method. Also, we give a numerical convergence order for the presented method in this part.

Keywords: Duffing fractional differential equations, Cubic Hermite spline functions, Caputo derivative, Operational matrix.

2020 Mathematics Subject Classification: 34A08, 65M70.

How to cite this article
M. Lakestani and R. Ghasemkhani, Solving linear and nonlinear Duffing fractional differential equations using cubic Hermite spline functions, *Math. Interdisc. Res.* **9** (4) (2024) 425-442.

*Corresponding author (E-mail: lakestani@tabrizu.ac.ir)
Academic Editor: Abbas Saadatmandi
Received 22 May 2024, Accepted 7 June 2024
DOI: 10.22052/MIR.2024.254944.1463

1. Introduction

The study of fractional derivatives, which speaks to extending differentiation to non-integer orders, has roots stretching back over three centuries. Although the idea was first discussed among notable mathematicians such as Leibniz and L'Hopital in the late 1600s, the systematic exploration of fractional calculus did not emerge until the 19th century. Pioneers such as Riemann and Liouville formulated foundational theories that formalized this concept, establishing a framework for understanding derivatives of arbitrary order. Fractional calculus has gained prominence due to its capacity to model complex systems that exhibit non-local, history-dependent behavior attributes often overlooked by traditional calculus, which relies on integer-order derivatives. This unique capability has made fractional derivatives indispensable in various scientific and engineering disciplines, including materials science, control systems, and biological processes. They enable more accurate descriptions of phenomena such as diffusion, wave propagation, and viscoelasticity, where memory effects play a significant role in dynamics.

Many problems in various fields of science and engineering lead to integrated boundary value problems (see [1, 2] for examples). In this paper, we want to solve a fractional boundary values problem (FBVP) in the form:

$$\begin{cases} y''(x) + c\ {}_*D_0^n y(x) + \mathsf{F}(x, y(x), y'(x)) = 0, \quad 0 < n < 1,\ x \in (0,1), c \in \mathbb{R} - \{0\}, \\ y(0) - a\ y'(0) = \int_0^1 h_1(s)y(s)ds, \quad y(1) - b\ y'(1) = \int_0^1 h_2(s)y(s)ds,\ \ a, b \in \mathbb{R}^+ \end{cases} \tag{1}$$

where $*D_0^n$ denotes the fractional derivative in the Caputo sense and h_1 and h_2 are given continuous functions.

Duffing equation is a nonlinear differential equation, discovered by electrical engineer German Duffing in the early 20th century and has named after him. This equation plays an important role in modeling many applications such as brain modeling, biological systems, disease prediction, orbit extraction, and so on (see [3–5]). The existence and uniqueness of the solutions for this equation can be found in [6, 7]. Although many numerical and analytical methods have been performed to solve the Duffing equation with two-point boundary conditions [8], less research has been done on the Duffing Equation (1). For example, the reproducing kernel space method [9, 10], the homotopy perturbation method, the reproducing kernel Hilbert space method [10], and the Legendre multiwavelets method [11] are being used for solving Equation (1).

Noori Dalawi et al. [12] have introduced an efficient algorithm based on the wavelet integration method to solve nonlinear fractional optimal control problems with inequality constraints. Also, for the first time, by using the interpolation properties of Hermitian cubic spline functions, they have constructed the operational matrix of the Caputo fractional derivative. Ashpazzadeh et al. [13], have used Cardinal Hermit's intrapolant multiscale function approximation method to solve nonlinear quadratic optimal control problems with inequality constraints. The authors in [14] have investigated the dynamics of infectious diseases using a fractional mathematical model based on Caputo's fractional derivatives, while Shahmorad et al. [15] employed a geometric approach for solving nonlinear fractional integro-differential equations. Bahmanpour et al. [16] utilized a Müntz wavelets collocation method to solve FDEs. Moreover, high-order and stable numerical algorithms with fractional spectral collocation method and with the help of space fractional derivative which is defined based on the Riesz derivative, have been developed in [17]. In addition, a finite element approach with cubic Hermite element was employed to solve a time fractional gas dynamics equation in [18]. Furthermore, Pourbabaee and Saadatmandi [19] solved distributed order FDEs using a collocation method based on Chebyshev polynomials. Also, in [20], the operational matrix of the fractional derivative and the operational matrix of the distributed order fractional derivative for Müntz-Legendre polynomials are found. For further research works on this problem, we recommend interested readers to refer to [21–27].

In this research, based on the work of [28], by using the operational matrix of fractional derivative for cubic Hermite spline functions (CHSFs) we expand the unknown function as a linear combination of CHSFs with unknown coefficients. Using CHSFs and collocation method we reduce the problem (1) to a system of algebraic equations which can be solved to find the unknown coefficients.

This paper is organized as follows: In Section 2, we give some preliminaries and definitions needed for our work. In Section 3, the numerical method is presented. Some numerical examples are presented to show the efficiency and validity of the method in Section 4. We finish the paper with a conclusion and suggesting ideas for future work.

2. Preliminaries and notations

2.1 The Caputo definition of fractional derivative and some other definitions

In this part, we will review the fundemental concepts and definitions of fractional calculus that will be used in the next sections.

Definition 2.1. ([29]). Let $n > 0$ be a real number. The Riemann-Liouville fractional integral operator of order n, denoted by J_a^n, is defined on $[a, b]$ and acts on functions $L^1[a, b]$ as:

$$J_a^n g(x) := \frac{1}{\Gamma(n)} \int_a^x (x-t)^{n-1} g(t)dt, \ a \le x \le b.$$

When $n = 0$ we define $J_0^n g(x) = g(x)$.

Definition 2.2. ([29]). Let $n \geq 0$ and $m = \lceil n \rceil$. The Caputo fractional derivative (CFD) of order n is defined as:

$$_*D_a^n g(x) = J_a^{m-n} D^m g(x),$$

when $D^m g \in L^1[a, b]$.
Applying Definition 2.1, we can write:

$$_*D_a^n g(x) = \frac{1}{\Gamma(m-n)} \int_a^x \frac{g^{(m)}(t)}{(x-t)^{m-n+1}} dt.$$

For the Caputo derivative we have:

$$_*D_a^n C = 0, \quad (C \text{ is a constant})$$

$$_*D_a^n x^\beta = \begin{cases} 0, & for\ \beta \in \mathbb{N}_0\ and\ \beta < \lceil n \rceil, \\ \frac{\Gamma(\beta+1)}{\Gamma(\beta+1-n)}\ x^{\beta-n}, & for\ \beta \in \mathbb{N}_0\ and\ \beta \geqslant \lceil n \rceil \quad or \quad \beta \notin \mathbb{N}\ and\ \beta > \lfloor n \rfloor. \end{cases}$$

Here, the ceiling function $\lceil n \rceil$ is the smallest integer greater than or equal to n and the floor function $\lfloor n \rfloor$ is the largest integer less than or equal to n.
$_*D_a^n$ is a linear operator, i.e.,

$$_*D_a^n \Big(c_1 f(x) + c_2 g(x) \Big) = c_1\ {_*D_a^n} f(x) + c_2\ {_*D_a^n} g(x),$$

where c_1 and c_2 are arbitrary constants.

Definition 2.3. ([30]). Let Ω be an open subset of $\mathbb{R}$. The Sobolev space of order s, denoted by $H^s(\Omega)$, is defined by:

$$H^s(\Omega) = \{g \in L^2(\Omega);\ g^{(m)} \in L^2(\Omega), m = 0, 1, \ldots, s,\ \ s \in \mathbb{N}\}.$$

The norm for $H^s(\Omega)$ is defined by

$$\|g\|_{s,\Omega} = \left(\sum_{m=0}^{s} \|g^{(m)}\|_{L^2(\Omega)} \right)^{\frac{1}{2}}.$$

Also, for the non-integer value $s \in (0, 1)$, the fractional Sobolev space is defined by [31]:

$$W^{s,2}(a, b) = \left\{ g \in L^2(a, b) : \frac{|g(x) - g(y)|}{|x-y|^{\frac{1}{2}+s}} \in L^2([a, b] \times [a, b]) \right\},$$

with the related norm

$$||g||_{W^{s,2}(a,b)} = \left[\int_a^b |g(x)|^2 dx + \int_a^b \int_a^b \frac{|g(x) - g(y)|^2}{|x-y|^{1+2s} dx dy} \right]^{\frac{1}{2}}.$$

2.2 Cubic Hermite spline functions on [0,1]

Cubic Hermite spline functions are defined by [32]

$$\phi_1(x) = \begin{cases} (x+1)^2(-2x+1), & x \in [-1,0], \\ (1-x)^2(2x+1), & x \in [0,1], \\ 0, & o.w., \end{cases} \tag{2}$$

$$\phi_2(x) = \begin{cases} (x+1)^2 x, & x \in [-1,0], \\ (1-x)^2 x, & x \in [0,1], \\ 0, & o.w., \end{cases} \tag{3}$$

and satisfy the following interpolation properties

$$\phi_1(k) = \delta_{0,k}, \quad \phi_1'(k) = 0, \quad \phi_2(k) = 0, \quad \phi_2'(k) = \delta_{0,k} \ (k \in \mathbb{Z}).$$

Here,

$$\delta_{i,k} = \begin{cases} 1, & i = k, \\ 0, & o.w. \end{cases}$$

The integer transformations of ϕ_1 and ϕ_2 form a basis for the space of C^1-continuous piecewise cubic functions on $\mathbb{R}$, which interpolate both the function values and their first derivatives at $k \in \mathbb{Z}$. For $l = 1,2$, it is possible to express any function in this space as a linear combination of $\phi_l(2^j x - k)$.
We put $\phi_l^{j,k}(x) = \phi_1(2^j x - k)$ for $l = 1,2$ and $B_{j,k} = supp\big[\phi_l^{j,k}(x)\big]$. It is easy to show that for $j,k \in \mathbb{Z}, B_{j,k} = \left[\frac{k-1}{2^j}, \frac{k+1}{2^j}\right]$. We also, define a set of indices as follows:

$$S_j = \big\{B_{j,k} \cap (0,1) \neq \emptyset\big\}, \quad j,k \in \mathbb{Z}.$$

It is evident that:

$$S_j = \big\{0,1,2,...,2^j\big\}, \quad j \in \mathbb{Z}.$$

We also need to define the cubic Hermite functions on the interval $[0,1]$. So, we introduce

$$\phi_l^{j,k}(x) = \phi_l^{j,k}(x).\chi_{[0,1]}(x), \quad j \in \mathbb{Z},\ k \in S_j,\ l = 1,2.$$

2.3 Function approximation

Let $\Phi_j(.)$ be $2(2^j+1)$ vector as:

$$\Phi_j(.) = \left[\phi_1^{j,0}(.), \phi_2^{j,0}(.), ..., \phi_1^{j,2^j}(.), \phi_2^{j,2^j}(.)\right]^T, \quad j \in \mathbb{Z}. \tag{4}$$

The interpolatory characteristics of the functions ϕ_1 and ϕ_2, allow for the to approximation of a function $g \in H^4[0,1]$ using cubic Hermite functions, when $j = J$

is fixed, as:

$$g(x) \simeq \sum_{k=0}^{2^J} \Big(c_{1,k}\ \phi_1^{J,k}(x) + c_{2,k}\ \phi_2^{J,k}(x) \Big) = C^T\ \Phi_J(x), \tag{5}$$

where

$$c_{1,k} = g(\frac{k}{2^J}),\ \ c_{2,k} = 2^{-J}\, g'(\frac{k}{2^J}), \quad k = 0, 1, \ldots, 2^J,$$

and C is a N-vector as:

$$C = \Big[c_{1,0},\ c_{2,0}, ..., c_{1,2^J},\ c_{2,2^J} \Big]^T,$$

where $N = 2(2^J + 1)$.

2.4 Ordinary and fractional derivative operational matrix

The ordinary derivatives of the functions $\phi_i(2^J x - \ell), \ell = 0, 1, 2, \ldots, 2^J, i = 1, 2$ can be approximated as:

$$\phi_i^{'}(2^J x - \ell) \simeq \sum_{k=0}^{2^J} \Big\{ \phi_i^{'}(k-\ell)\phi_1(2^J x - k) + \frac{1}{2^J}\phi_i^{''}(x)\big|_{x=k-\ell}\ \phi_2(2^J x - k) \Big\} \tag{6}$$

$$\phi_i^{''}(2^J x - \ell) \simeq \sum_{k=0}^{2^J} \Big\{ \phi_i^{''}(k-\ell)\phi_1(2^J x - k) + \frac{1}{2^J}\phi_i^{'''}(x)\big|_{x=k-\ell}\ \phi_2(2^J x - k) \Big\} \tag{7}$$

Using the relations (6) and (7) we can find ordinary derivatives of the first and second order for the vector function Φ_J in the form:

$$\Phi_J'(x) \simeq D_\Phi\, .\Phi_J(x), \tag{8}$$

$$\Phi_J''(x) \simeq D_\Phi^2\, .\Phi_J(x). \tag{9}$$

Here, D_Φ is the $N \times N$ (six-diagonal matrix) operational matrix of ordinary derivative, which is defined in [32].

Also, CFD of the functions $\phi_i(2^J x - \ell)$, of order $n, (0 < n < 1)$ may be approximated as:

$$\begin{aligned} &{}_*D_0^n \phi_i(2^J x - \ell) \\ &\simeq \sum_{k=0}^{2^J} \Big\{ {}_*D_0^n \phi_i(k-\ell)\phi_1(2^J x - k) + \frac{1}{2^J} D\big({}_*D_0^n \phi_i(x)\big)\big|_{x=k-\ell}\ \phi_2(2^J x - k) \Big\}, \\ &\qquad \ell = 0, 1, \ldots, 2^J,\ \ i = 1, 2. \end{aligned} \tag{10}$$

Here, D represents the first order classical derivative. Employing Equation (10) we find the CFD of order n for the vector function Φ_J as:

$$ {}_{*}D_0^n \Phi_J(x) \simeq \mathcal{D}_n \, \Phi_J(x), \tag{11} $$

where $\mathcal{D}_n$ is the $N \times N$ operational matrix of fractional derivative. For $J = 0$ and $n = \frac{1}{10}$, the matrix $\mathcal{D}_n$ is as follows:

$$ \mathcal{D}_n = \begin{pmatrix} 0 & 0 & \frac{-600}{551\Gamma(\frac{9}{10})} & \frac{20}{57\Gamma(\frac{9}{10})} \\ 0 & 0 & \frac{-10}{551\Gamma(\frac{9}{10})} & \frac{11}{171\Gamma(\frac{9}{10})} \\ 0 & 0 & \frac{600}{551\Gamma(\frac{9}{10})} & \frac{-20}{57\Gamma(\frac{9}{10})} \\ 0 & 0 & \frac{200}{4959\Gamma(\frac{9}{10})} & \frac{220}{171\Gamma(\frac{9}{10})} \end{pmatrix}. $$

3. Description of numerical method

In this section, we solve the FBVP (1) by applying cubic Hermite spline functions. First, we approximate unknown functions y and h_i $(i = 1, 2)$ in the problem (1), by using Equation (5), as:

$$ y(x) \simeq y_J(x) = \sum_{k=0}^{2^J} \left\{ Y_{1,k} \ \phi_1^{J,k}(x) + Y_{2,k} \ \phi_2^{J,k}(x) \right\} = Y^T \Phi_J(x), \tag{12} $$

$$ h_i(x) \simeq h_{iJ}(x) = \sum_{k=0}^{2^J} \left\{ H^i_{1,k} \ \phi_1^{J,k}(x) + H^i_{2,k} \ \phi_2^{J,k}(x) \right\} = {H^i}^T \Phi_J(x), \tag{13} $$

where Y and H^i are the following unknown vectors:

$$ Y = \left[Y_{1,0}, Y_{2,0}, Y_{1,1}, Y_{2,1}, \ldots, Y_{1,2^J}, Y_{2,2^J} \right]^T, $$

$$ H^i = \left[H^i_{1,0}, H^i_{2,0}, H^i_{1,1}, H^i_{2,1}, \ldots, H^i_{1,2^J}, H^i_{2,2^J} \right]^T. $$

Moreover, using the operational matrices in Equations (8), (9) and (11), we can approximate $y'(x), y''(x)$ and ${}_{*}D_0^n y(x)$ as:

$$ y'(x) \simeq Y^T \Phi'_J(x) \simeq Y^T D_\Phi \Phi_J(x), \tag{14} $$

$$ y''(x) \simeq Y^T \Phi''_J(x) \simeq Y^T D_\Phi^2 \Phi_J(x), \tag{15} $$

$$ {}_{*}D_0^n y(x) \simeq {}_{*}D_0^n Y^T \Phi_J(x) \simeq Y^T \mathcal{D}_n \Phi_J(x). \tag{16} $$

Employing Equations (14), (15), (16) and Equation (1), we obtain:

$$Y^T D_\Phi^2 \Phi_J(x) + Y^T \mathcal{D}_n \Phi_J(x) + \mathsf{F}\big(x, Y^T \Phi_J(x), Y^T D_\Phi \Phi_J(x)\big) \simeq 0, \quad 0 < x < 1. \tag{17}$$

Also by replacing (12), (13) and (14) in the integral boundary conditions (1), we get:

$$Y^T \Phi_J(0) - a\, Y^T D_\Phi\, \Phi_J(0) = H^{1^T}\Big(\int_0^1 \Phi_J(s)\, \Phi_J^T(s) ds\Big) Y, \tag{18}$$

$$Y^T \Phi_J(1) - b\, Y^T D_\Phi\, \Phi_J(1) = H^{2^T}\Big(\int_0^1 \Phi_J(s)\, \Phi_J^T(s) ds\Big) Y, \tag{19}$$

where $\int_0^1 \Phi_J(s)\, \Phi_J^T(s) ds$ is defined as the following $N \times N$ (seven-diagonal matrix):

$$\begin{pmatrix} A_1 & B_1 & & & & \\ B_2 & C & B_1 & & & \\ & B_2 & C & B_1 & & \\ & & \ddots & \ddots & \ddots & \\ & & & B_2 & C & B_1 \\ & & & & B_2 & A_2 \end{pmatrix},$$

in which

$$A_1 = \begin{pmatrix} 26 & \frac{11}{3} \\ \frac{11}{3} & \frac{2}{3} \end{pmatrix}, \quad A_2 = \begin{pmatrix} 26 & -\frac{11}{3} \\ -\frac{11}{3} & \frac{2}{3} \end{pmatrix}, \quad B_1 = \begin{pmatrix} 9 & -\frac{13}{6} \\ \frac{13}{6} & -\frac{1}{2} \end{pmatrix}, \quad B_2 = \begin{pmatrix} 9 & \frac{13}{6} \\ -\frac{13}{6} & -\frac{1}{2} \end{pmatrix},$$

and

$$C = \begin{pmatrix} 52 & 0 \\ 0 & \frac{4}{3} \end{pmatrix}.$$

By collocating Equation (17) at $N-2$ equally spaced nodes $x_i \in [0, 1]$, for $i = 1, 2, ..., N-2$, we have:

$$Y^T D_\Phi^2\, \Phi_J(x_i) + Y^T \mathcal{D}_n\, \Phi_J(x_i) + \mathsf{F}\big(x_i, Y^T \Phi_J(x_i), Y^T D_\Phi\, \Phi_J(x_i)\big) \simeq 0. \tag{20}$$

The combition of Equation (20) with Equations (18) and (19) creates a system of algebraic equations that consist of N equations and N unknowns. This system can be solve to obtain the unknown vector Y. Therefore, the solution y of problem (1) can be found.

4. Numerical examples

Now, we apply the method described in the previous section to solve some examples.

For various levels of J, we tabulate L_∞ and L_2 errors. We assume $e_J(\mathtt{x}) = O(2^{-pJ})$, and solve for p accordingly

$$p = \log_2 \frac{\|e_{J-1}(x)\|_{L^\infty([0,1])}}{\|e_J(x)\|_{L^\infty([0,1])}}. \tag{21}$$

Example 4.1. For $n \in (0,1)$, we consider the following nonlinear problem

$$y''(x) + {}_*D_0^n y(x) + y(x)cos(y(x)) = f(x), \;\; x \in (0,1),$$

with integral boundary conditions(IBCs):

$$\begin{cases} y(0) - 2y'(0) = \int_0^1 -xy(x)dx, \\ y(1) + \frac{12}{25}y'(1) = \int_0^1 2(1+x)y(x)dx, \end{cases}$$

where

$$f(x) = 12x^2 + \frac{120}{\Gamma(5-n)}x^{4-n} + \frac{1}{\Gamma(2-n)}x^{1-n} + (1+x+x^4)cos(1+x+x^4),$$

and the exact solution is $y(x) = 1 + x + x^4$.

In Table 1, we report the L_∞ and L_2 errors for various values of n and J. Moreover, Table 1 shows the numerical convergence order for different values of n and J. Furthermore, the graph of absolute error functions $|y(x) - y_J(x)|$ for $n = 0.5, 0.6, 0.7, 0.8, 0.9$ and $J = 6$ are given in Figure 1.

It is clear that the exact solution lies in $H^4[0,1]$. The obtained results show that the numerical order of convergence (21) is as $O(2^{-pJ})$, where p is close to 4.

Example 4.2. As an other example, for $n \in (0,1)$, we consider the following FBVP

$$y''(x) + {}_*D_0^n y(x) - 5ny(x) = f(x), \; x \in (0,1),$$

with IBCs

$$\begin{cases} \frac{5}{6}y(0) + \frac{1}{5n+2}y'(0) = \int_0^1 xy(x)dx, \\ \frac{7}{36}y(1) + \frac{1}{(5n+1)(5n+3)}y'(1) = \int_0^1 x^2y(x)dx, \end{cases}$$

where

$$f(x) = 5n(5n-1)x^{5n-2} + \frac{\Gamma(5n+1)}{\Gamma(4n+1)}x^{4n} + \frac{1}{\Gamma(2-n)}x^{1-n} - 5nx^{5n} - 5nx - 5n.$$

Table 1: L_∞ and L_2 errors for $y(x)$ using presented method for Example 4.1.

	J	L_∞ error	L_2 error	p
	2	7.73×10^{-2}	4.49×10^{-2}	
	3	1.92×10^{-2}	1.10×10^{-2}	4.02
	4	4.81×10^{-3}	2.73×10^{-3}	3.99
$n = 0.5$	5	1.20×10^{-3}	6.82×10^{-4}	4.00
	6	3.20×10^{-4}	1.81×10^{-4}	3.75
	7	8.01×10^{-5}	4.53×10^{-5}	3.99
	2	7.32×10^{-2}	4.25×10^{-2}	
	3	1.81×10^{-2}	1.03×10^{-2}	4.04
	4	4.52×10^{-3}	2.57×10^{-3}	4.00
$n = 0.7$	5	1.12×10^{-3}	6.40×10^{-4}	4.03
	6	2.82×10^{-4}	1.59×10^{-4}	3.97
	7	7.05×10^{-5}	3.99×10^{-5}	4.00
	2	6.66×10^{-2}	3.87×10^{-2}	
	3	1.62×10^{-2}	9.30×10^{-2}	4.11
	4	4.01×10^{-3}	2.28×10^{-3}	4.03
$n = 0.9$	5	9.99×10^{-4}	5.61×10^{-4}	4.01
	6	2.49×10^{-4}	1.41×10^{-4}	4.01
	7	6.22×10^{-5}	3.52×10^{-5}	4.00

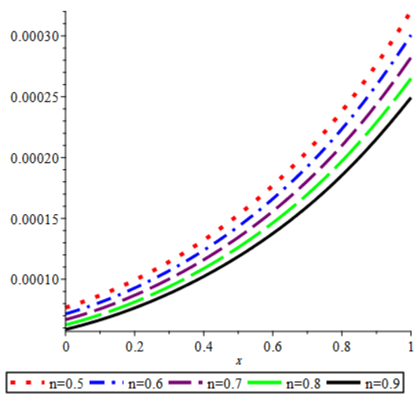

Figure 1: The graph of absolute error functions $|y(x) - y_J(x)|$ with $n = 0.5, 0.6, 0.7, 0.8, 0.9$ and $J = 6$, for Example 4.1.

Table 2: L_∞ and L_2 errors for $y(x)$ using presented method, for Example 4.2 .

	J	L_∞ error	L_2 error	p
	2	2.10×10^{-1}	1.29×10^{-1}	
	3	4.09×10^{-2}	2.53×10^{-2}	5.13
	4	8.32×10^{-3}	5.17×10^{-3}	4.91
$n = 0.7$	5	1.80×10^{-3}	1.12×10^{-3}	4.62
	6	4.10×10^{-4}	2.57×10^{-4}	4.39
	7	9.67×10^{-5}	6.07×10^{-5}	4.23
	2	3.42×10^{-1}	2.06×10^{-1}	
	3	7.99×10^{-2}	4.83×10^{-2}	4.28
	4	1.89×10^{-2}	1.14×10^{-2}	4.22
$n = 0.8$	5	4.59×10^{-3}	2.78×10^{-3}	4.11
	6	1.13×10^{-3}	6.84×10^{-4}	4.06
	7	2.80×10^{-4}	1.69×10^{-4}	4.03
	2	4.70×10^{-1}	2.78×10^{-1}	
	3	1.18×10^{-1}	6.98×10^{-2}	3.98
	4	2.90×10^{-2}	1.71×10^{-2}	4.06
$n = 0.9$	5	7.17×10^{-3}	4.24×10^{-3}	4.04
	6	1.78×10^{-3}	1.05×10^{-3}	4.02
	7	4.43×10^{-4}	2.62×10^{-4}	4.01

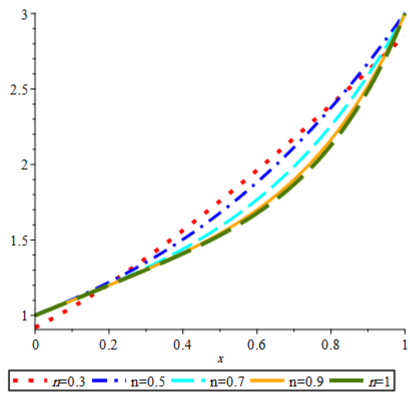

Figure 2: Comparison of $y(x)$ for $J = 6$ and $n = 0.3, 0.5, 0.7, 0.9$ and the exact solution for $n = 1$, for Example 4.2.

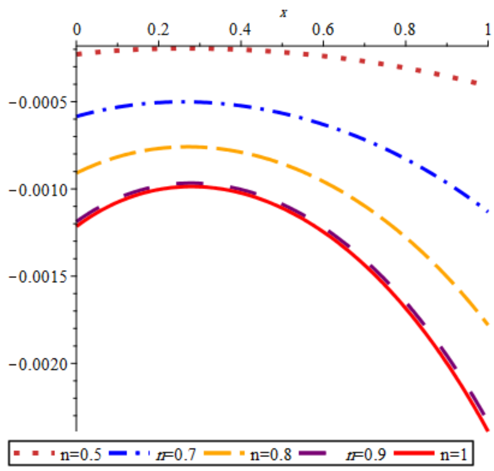

Figure 3: The graph of absolute error functions $|y(x) - y_J(x)|$ for $J = 6$ and $n = 0.5, 0.7, 0.8, 0.9, 1$, for Example 4.2.

The exact solution of this problem is $y(x) = 1 + x + x^{5n}$.

We provide the results for L_∞ and L_2 errors for various values of J and n in Table 2. Also, we plot the numerical solutions for $y(x)$ with $J = 6$ and $n = 0.3, 0.5, 0.7, 0.9, 1$ in Figure 2 and absolute error functions $|y(x) - y_J(x)|$ for $n = 0.5, 0.7, 0.8, 0.9, 1$ and $J = 6$ in Figure 3.

Example 4.3. For $n \in (0, 1)$, consider the following FBVP

$$y''(x) + {}_*D_0^n y(x) - 2y(x) = f(x),\ x \in (0, 1),$$

with IBCs

$$\begin{cases} \frac{1}{3n+1} y(0) - y'(0) = \int_0^1 y(x)dx, \\ \frac{1}{4} y(1) + \frac{1}{3n(3n+2)} y'(1) = \int_0^1 xy(x)dx, \end{cases}$$

where

$$f(x) = 3n(3n-1)x^{3n-2} + \frac{\Gamma(3n+1)}{\Gamma(2n+1)} x^{2n} - 2x^{3n} - 2.$$

The exact solution of this problem is $y(x) = 1 + x^{3n}$.

We report the L_∞ and L_2 errors for different values of $n = 0.5, 0.6, 0.7, 0, 8$ and J in Table 3. For the cases $3n = 1.5, 1.8, 2.1, 2.4$, the exact solutions approach to $W^{3n,2}[0, 1]$.

Example 4.4. As the last example, for $n \in (0, 1)$ we consider the following FBVP

$$y''(x) + {}_*D_0^n y(x) + (x - x^2)y^3(x) = f(x),\ x \in (0, 1), \tag{22}$$

Table 3: L_∞ and L_2 errors for $y(x)$ using presented method, for Example 4.3 .

	J	L_∞ error	L_2 error	p
	2	9.01×10^{-1}	6.98×10^{-1}	
	3	3.78×10^{-1}	2.99×10^{-1}	2.38
	4	1.79×10^{-1}	1.44×10^{-1}	2.11
$n = 0.5$	5	9.63×10^{-2}	7.85×10^{-2}	1.85
	6	5.75×10^{-2}	4.73×10^{-2}	1.67
	7	3.69×10^{-2}	3.05×10^{-2}	1.55
	2	7.42×10^{-1}	5.36×10^{-1}	
	3	2.67×10^{-1}	1.94×10^{-1}	2.77
	4	1.10×10^{-1}	8.05×10^{-2}	2.42
$n = 0.6$	5	5.14×10^{-2}	3.75×10^{-2}	2.14
	6	2.61×10^{-2}	1.91×10^{-2}	1.96
	7	1.60×10^{-2}	1.02×10^{-2}	1.86
	2	7.86×10^{-2}	5.31×10^{-2}	
	3	2.59×10^{-2}	1.73×10^{-2}	3.03
	4	9.48×10^{-3}	6.32×10^{-3}	2.73
$n = 0.7$	5	3.79×10^{-3}	2.52×10^{-3}	2.50
	6	1.55×10^{-3}	9.24×10^{-4}	2.44
	7	7.19×10^{-4}	4.77×10^{-4}	2.15
	2	5.77×10^{-2}	3.68×10^{-2}	
	3	1.69×10^{-2}	1.06×10^{-2}	3.41
	4	5.42×10^{-3}	3.38×10^{-3}	3.11
$n = 0.8$	5	1.84×10^{-3}	1.14×10^{-3}	2.94
	6	6.56×10^{-4}	4.07×10^{-4}	2.80
	7	2.39×10^{-4}	1.48×10^{-4}	2.74

with IBCs

$$\begin{cases} y(0) - \frac{2}{\pi^2} y'(0) = \int_0^1 -y(x)dx, \\ y(1) + \frac{1}{\pi^2} y'(1) = \int_0^1 -xy(x)dx, \end{cases}$$

where

$$f(x) = -sin(\pi x)(\pi^2 + (x^2 - x)sin^2(\pi x) + \pi cos(\pi x),$$

The exact solutions for the values of $n \neq 1$ are not exist. The approximate solutions obtained by the present method for various values of $n = 0.5, 0.7, 0.8, 0.9$ and 1 are plotted in Figure 4, which shows that as n tends to 1, the approximate solutions approaches to the plot of $y(x) = sin(\pi x)$.

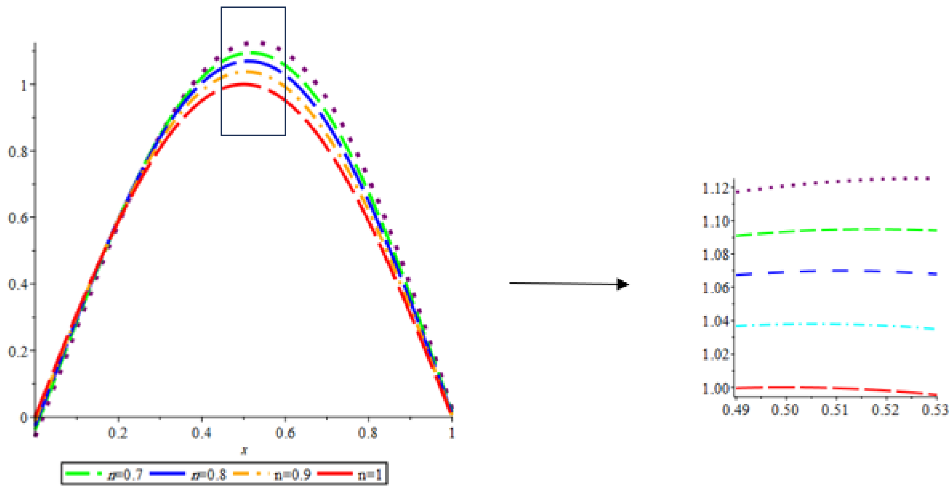

Figure 4: Plot of approximate solutions for $n = 0.5, 0.7, 0.8, 0.9$, and 1, for Example 4 .

5. Conclusion

In this study, we employ cubic Hermite spline functions to address nonlinear Duffing fractional differential equations subject to integral boundary conditions. The operational matrix associated with the Caputo-type fractional derivative, along with the collocation method, was utilized to derive the solution. Our findings indicate that the proposed method demonstrates a strong correlation with the numerical order of convergence when the exact solution is in $H^4[0, 1]$. However, when the exact solution is in the fractional Sobolev space $W^{s,2}(0, 1)$, where $1 \leq s < 4$, we see a decrease in the convergence order to $O(2^{-sJ})$. Future research may aim to theoretically establish the convergence order of our method within the framework of fractional Sobolev spaces.

Conflicts of Interest. The authors declare that they have no conflicts of interest regarding the publication of this article.

References

[1] B. Ahmad, S. K. Ntouyas and A. Alsaedi, On a coupled system of fractional differential equations with coupled nonlocal and integral boundary conditions, *Chaos Solitons Fractals* **83** (2016) 234 – 241, https://doi.org/10.1016/j.chaos.2015.12.014.

[2] M. R. Doostdar, M. Kazemi and A. Vahidi, A numerical method for solving the Duffing equation involving both integral and non-integral forcing terms with separated and integral boundary conditions, *Comput. Methods Differ. Equ.* **11** (2023) 241 – 253, https://doi.org/ 10.22034/CMDE.2022.50054.2082.

[3] M. Chai and L. Ba, Application of EEG signal recognition method based on Duffing equation in psychological stress analysis, *Adv. Math. Phys.* **2021** (2021) #1454547, https://doi.org/10.1155/2021/1454547.

[4] A. A. Cherevko, E. E. Bord, A. K. Khe, V. A. Panarin and K. J. Orlov, The analysis of solutions behaviour of Van der Pol Duffing equation describing local brain hemodynamics, *J. Phys.: Conf. Ser.* **894** (2017) #012012, https://doi.org/10.1088/1742-6596/894/1/012012.

[5] R. Srebro, The Duffing oscillator: a model for the dynamics of the neuronal groups comprising the transient evoked potential, *Electroencephalogr. Clin. Neurophysiol.* **96** (1995) 561 – 573, https://doi.org/10.1016/0013-4694(95)00088-G.

[6] B. Ahmad and A. Alsaedi, Existence of approximate solutions of the forced Duffing equation with discontinuous type integral boundary conditions, *Nonlinear Anal. Real World Appl.* **10** (2009) 358 – 367, https://doi.org/10.1016/j.nonrwa.2007.09.004.

[7] A. Boucherif, Second-order boundary value problems with integral boundary conditions, *Nonlinear Anal. Theory Methods Appl.* **70** (2009) 364 – 371, https://doi.org/10.1016/j.na.2007.12.007.

[8] A. Saadatmandi and S. Yeganeh, New approach for the Duffing equation involving both integral and non-integral forcing terms, *Politehn. Univ. Bucharest Sci. Bull. Ser. A Appl. Math. Phys.* **79** (2017) 46 – 52.

[9] Z. Chen, W. Jiang and H. Du, A new reproducing kernel method for Duffing equations, *Int. J. Comput. Math.* **98** (2021) 2341 – 2354, https://doi.org/10.1080/00207160.2021.1897111.

[10] F. Deutsch, *Best Approximation in Inner Product Spaces*, Springer, New York, 2001.

[11] S. Mashayekhi, Y. Ordokhani and M. Razzaghi, A hybrid functions approach for the Duffing equation, *Phys. Scr.* **88** (2013) #025002, https://doi.org/10.1088/0031-8949/88/02/025002.

[12] A. Noori Dalawi, M. Lakestani and E. Ashpazzadeh, An efficient algorithm for the multi-scale solution of nonlinear fractional optimal control problems, *Mathematics* **10** (2022) #3779, https://doi.org/10.3390/math10203779.

[13] E. Ashpazzadeh, M. Lakestani and M.Razzaghi, Nonlinear constrained optimal control problems and cardinal Hermite interpolant multiscaling functions, *Asian J. Control.* **20** (2018) 558 – 567, https://doi.org/10.1002/asjc.1526.

[14] R. Akbari and L. Navaei, Fractional dynamics of infectious disease transmission with optimal control, *Math. Interdisc. Res.* **9** (2024) 199 – 213, https://doi.org/10.22052/MIR.2023.253000.1410.

[15] S. Shahmorad, S. Pashaei and M. S. Hashemi, Numerical solution of a nonlinear fractional integro-differential equation by a geometric approach, *Differ. Equ. Dyn. Syst.* **29** (2021) 585 – 596, https://doi.org/10.1007/s12591-017-0395-1.

[16] M. Bahmanpour, M. Tavassoli-Kajani and M. Maleki, A Müntz wavelets collocation method for solving fractional differential equations, *Comput. Appl. Math.* **37** (2018) 5514 – 5526.

[17] M. Abbaszadeh, A. Bagheri Salec, S. Kamel and A. Al-Khafaji, The effect of fractional-order derivative for pattern formation of Brusselator reaction–diffusion model occurring in chemical reactions, *Iranian J. Math. Chem.* **14** (2023) 243 – 269, https://doi.org/10.22052/IJMC.2023.253498.1759.

[18] M. A. Shallal, A. H. Taqi, H. N. Jabbar, H. Rezazadeh, B. F. Jumaa, A. Korkmaz and A. Bekir, A numerical technique of the time fractional gas dynamics equation using finite element approach with cubic Hermit element, *Appl. Comput. Math.* **21** (2022) 269 – 278.

[19] M. Pourbabaee and A. Saadatmandi, Collocation method based on Chebyshev polynomials for solving distributed order fractional differential equations, *Comput. Methods Differ. Equ.* **9** (2021) 858 – 873, https://doi.org/10.22034/CMDE.2020.38506.1695.

[20] M. Pourbabaee and A. Saadatmandi, A new operational matrix based on Müntz–Legendre polynomials for solving distributed order fractional differential equations, *Math. Comput. Simulation* **194** (2022) 210 – 235, https://doi.org/10.1016/j.matcom.2021.11.023.

[21] A. Abedini, K. Ivaz, S. Shahmorad and A. Dadvand, Numerical solution of the time-fractional Navier-Stokes equations for incompressible flow in a lid-driven cavity, *Comput. Appl. Math.* **40** (2021) #34, https://doi.org/10.1007/s40314-021-01413-w.

[22] E. Ashpazzadeh, M. Lakestani and A. Fatholahzadeh, Spectral methods combined with operational matrices for fractional optimal control problems: a review, *Appl. Comput. Math.* **20** (2021) 209 – 235.

[23] S. Bonyadi, Y. Mahmoudi, M. Lakestani and M. Jahangiri rad, Numerical solution of space-time fractional PDEs with variable coefficients using shifted Jacobi collocation method, *Comput. Methods Differ. Equ.* **11** (2023) 81 – 94, https://doi.org/10.22034/CMDE.2022.49901.2077.

[24] H. Fazli, F. Bahrami and S. Shahmorad, Extremal solutions for multi-term nonlinear fractional differential equations with nonlinear boundary conditions, *Comput. Methods Differ. Equ.* **11** (2023) 32 – 41, https://doi.org/10.22034/CMDE.2021.48310.2018.

[25] M. N. Oqielat, T. Eriqat, Z. Al-Zhour, A. El-Ajou and S. Momani, Numerical solutions of time-fractional nonlinear water wave partial differential equation via Caputo fractional derivative: an effective analytical method and some applications, *Appl. Comput. Math.* **21** (2022) 207 – 222.

[26] F. Nourian, M. Lakestani, S. Sabermahani and Y. Ordokhani, Touchard wavelet technique for solving time-fractional Black Scholes model, *Comp. Appl. Math.* **41** (2022) #150, https://doi.org/10.1007/s40314-022-01853-y.

[27] F. Shariffar, A. H. R. Sheikhani and M. Mashoof, Numerical analysis of fractional differential equation by TSI-wavelet method, *Comput. Methods Differ. Equ.* **9** (2021) 659 – 669, https://doi.org/10.22034/CMDE.2020.29679.1429.

[28] A. Ghasemi and A. Saadatmandi, A new Bernstein-reproducing kernel method for solving forced Duffing equations with integral boundary conditions, *Comput. Methods Differ. Equ.* **12** (2024) 329 – 337, https://doi.org/10.22034/cmde.2023.57413.2401.

[29] K. Diethelm, *The Analysis of Fractional Differential Equations*, Springer-Verlag Berlin Heidelberg 2010.

[30] V. Mazja, *Sobolev Spaces*, Springer Berlin, Heidelberg, 1985.

[31] M. Bergounioux, A. Leaci, G. Nardi and F. Tomarelli, Fractional Sobolev spaces and functions of bounded variation of one variable, *Fract. Calc. Appl. Anal.* **20** (2017) 936 – 962, https://doi.org/10.1515/fca-2017-0049.

[32] R. Mohammadzadeh, M. Lakestani and M. Dehghan, Collocation method for the numerical solutions of Lane-Emden type equations using cubic Hermite spline functions, *Math. Methods Appl. Sci.* **37** (2014) 1303 – 1317, https://doi.org/10.1002/mma.2890.

Mehrdad Lakestani
Department of Mathematics,
Faculty of Mathematics, Statistics and Computer Science,
University of Tabriz,
Tabriz, I. R. Iran
e-mail: lakestani@tabrizu.ac.ir

Roya Ghasemkhani
Department of Mathematics,
Faculty of Science,
University of Jiroft,
Jiroft, I. R. Iran
e-mail: roya.ghasemkhani@gmail.com